AREA ATTENTION

Yang Li
Google Research
Mountain View, CA 94043, USA
`liyang@google.com`

Lukasz Kaiser
Google Brain
Mountain View, CA 94043, USA
`lukaszkaiser@google.com`

Samy Bengio
Google Brain
Mountain View, CA 94043, USA
`bengio@google.com`

Si Si
Google Research
Mountain View, CA 94043, USA
`sisidaisy@google.com`

ABSTRACT

Existing attention mechanisms, are mostly item-based in that a model is designed to attend to a single item in a collection of items (the memory). Intuitively, an area in the memory that may contain multiple items can be worth attending to as a whole. We propose area attention: a way to attend to an area of the memory, where each area contains a group of items that are either spatially adjacent when the memory has a 2-dimensional structure, such as images, or temporally adjacent for 1-dimensional memory, such as natural language sentences. Importantly, the size of an area, i.e., the number of items in an area, can vary depending on the learned coherence of the adjacent items. By giving the model the option to attend to an area of items, instead of only a single item, we hope attention mechanisms can better capture the nature of the task. Area attention can work along multi-head attention for attending to multiple areas in the memory. We evaluate area attention on two tasks: neural machine translation and image captioning, and improve upon strong (state-of-the-art) baselines in both cases. These improvements are obtainable with a basic form of area attention that is parameter free. In addition to proposing the novel concept of area attention, we contribute an efficient way for computing it by leveraging the technique of summed area tables.

1 INTRODUCTION

Attentional mechanisms have significantly boosted the accuracy on a variety of deep learning tasks (Bahdanau et al., 2014; Luong et al., 2015; Xu et al., 2015). They allow the model to selectively focus on specific pieces of information, which can be a word in a sentence for neural machine translation (Bahdanau et al., 2014; Luong et al., 2015) or a region of pixels in image captioning (Xu et al., 2015; Sharma et al., 2018).

An attentional mechanism typically follows a *memory-query* paradigm, where the memory M contains a collection of items of information from a source modality such as the embeddings of an image or the hidden states of encoding an input sentence, and the query q comes from a target modality such as the hidden state of a decoder model. In recent architectures such as Transformer (Vaswani et al., 2017), self-attention involves queries and memory from the same modality for either encoder or decoder. Each item in the memory has a key and value (k_i, v_i), where the key is used to compute the probability a_i regarding how well the query matches the item (see Equation 1).

$$a_i = \frac{\exp(f_{att}(q, k_i))}{\sum_{j=1}^{|M|} \exp(f_{att}(q, k_j))} \tag{1}$$

The typical choices for f_{att} include dot products qk_i (Luong et al., 2015) and a multilayer perceptron (Bahdanau et al., 2014). The output O_q^M from querying the memory M with q is then calculated as the sum of all the values in the memory weighted by their probabilities (see Equation 2), which can be fed to other parts of the model for further calculation. During training, the model learns to attend

1

to specific piece of information, e.g., the correspondance between a word in the target sentence and a word in the source sentence for translation tasks.

$$O_q^M = \sum_{i=1}^{|M|} a_i v_i \qquad (2)$$

Attention mechanisms are typically designed to focus on a single item in the entire memory, where each item defines the granularity of what the model can attend to. For example, it can be a character for a character-level translation model, a word for a word-level model or a grid cell for an image-based model. Such a construction of attention granularity is predetermined rather than learned. While this kind of single-item attention has been helpful for many tasks, it is fundamentally limited for modeling complex attention distribution that might be involved in a task.

To combat this issue, multi-head attention (Vaswani et al., 2017) allows a model to attend multiple items at the same time where each head captures a different aspect of the task, although each head is still single-item-based attention. More recently, (Pedersoli et al., 2016) proposed mechanisms for attending to objects in images for captioning tasks, which employ dedicated sub networks for detecting objects in the scene. In this paper, we propose *area attention*, as a general mechanism for the model to attend to a group of items in the memory that are structurally adjacent. In area attention, each unit for attention calculation is an area that can have one or more than one item. Each of these areas can have a varying number of items that allow the model to capture rich alignment distributions—thus the granularity of attention is learned from the data. Note that area attention subsumes single-item attention because when an area contains a single item it is equivalent to single-item attention. Area attention is complementary to multi-head attention. With each head using area attention, multi-head area attention allows the model to attend to multiple areas. As we show in the experiments, the combination of both achieved the best results.

We evaluated area attention on two tasks: machine translation on both English to German and English to French (Wu et al., 2016; Lee et al., 2016), and image captioning (Sharma et al., 2018). These tasks involve multiple model architectures, including the canonical LSTM seq2seq with attention (Luong et al., 2015) and the encoder-decoder Transformer (Vaswani et al., 2017).

2   AREA-BASED ATTENTION MECHANISMS

An area is a group of structurally adjacent items in the memory. When the memory consists of a sequence of items, a 1-dimensional structure, an area is a range of items that are sequentially (or temporally) adjacent and the number of items in the area can be one or multiple. Many language-related tasks are categorized in the 1-dimensional case, e.g., machine translation or sequence prediction tasks. In Figure 1, the original memory is a 4-item sequence. By combining the adjacent items in the sequence, we form area memory where each item is a combination of multiple adjacent items in the original memory. We can limit the maximum area size to consider for a task. In Figure 1, the maximum area size is 3.

When the memory contains a grid of items, a 2-dimensional structure, an area can be any rectangular region in the grid (see Figure 2). This resembles many image-related tasks, e.g., image captioning. Again, we can limit the maximum size allowed for an area. For a 2-dimensional area, we can set the maximum height and width for each area. In this example, the original memory is a 3x3 grid of items and the maximum height and width allowed for each area is 2.

As we can see, many areas can be generated by combining adjacent items. For the 1-dimensional case, the number of areas that can be generated is $|R| = (L - S)S + (S + 1)S/2$ where S is the maximum size of an area and L is the length of the sequence. For the 2-dimensional case, there are an quadratic number of areas can be generated from the original memory: $|R| = |R_v||R_h|$. $|R_v| = (L_v - H)H + (H + 1)H/2$ and $|R_h| = (L_h - W)W + (W + 1)W/2$ where L_v and L_h are the height and width of the memory grid and H and W are the maximum height and width allowed for a rectangular area.
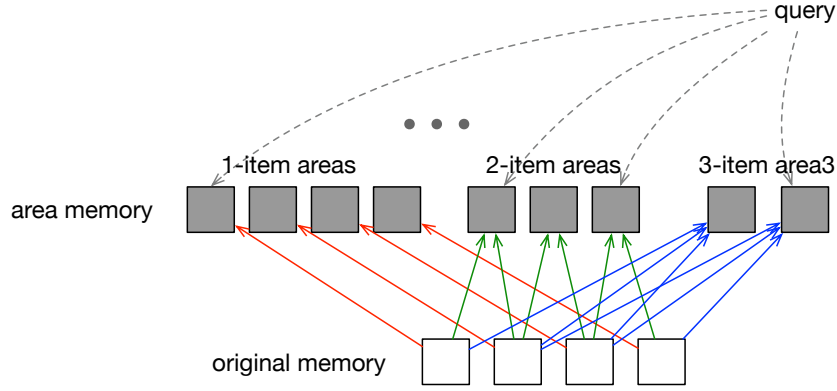
Figure 1: An illustration of area attention for the 1-dimensional case. In this example, the memory is a 4-item sequence and the maximum size of an area allowed is 3.
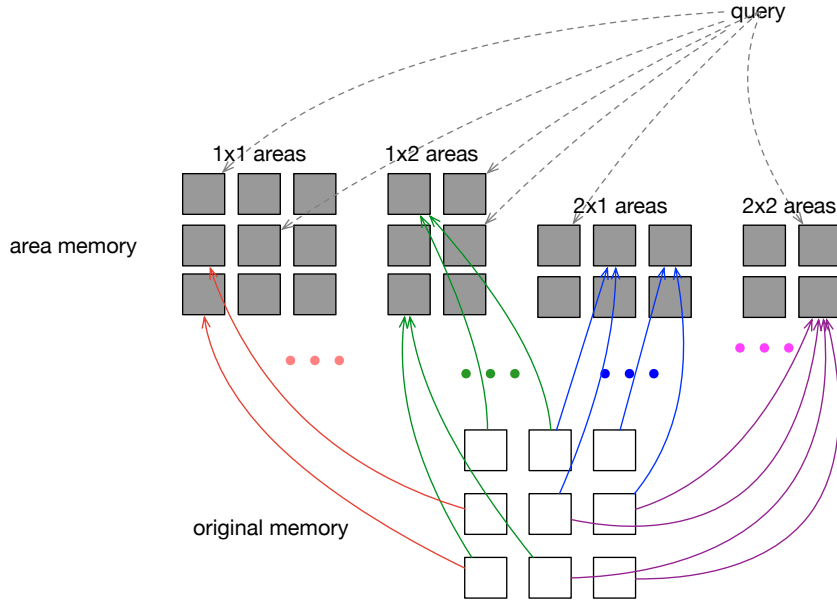

Figure 2: An illustration of area attention for the 2-dimensional case. In this example, the memory is a 3x3 grid and the dimension allowed for an area is 2x2.

To be able to attend to each area, we need to define the key and value for each area that contains one or multiple items in the original memory. As the first step to explore area attention, we define the key of an area, μ_i, simply as the mean vector of the key of each item in the area.

$$\mu_i = \frac{1}{|r_i|} \sum_{j=1}^{|r_i|} k_{i,j} \qquad (3)$$

where $|r_i|$ is the size of the area r_i. For the value of an area, we simply define it as the the sum of all the value vectors in the area.

$$v_i^{r_i} = \sum_{j=1}^{|r_i|} v_{i,j} \qquad (4)$$

3

With the keys and values defined, we can use the standard way for calculating attention as discussed in Equation 1 and Equation 2. Note that this basic form of area attention is parameter-free—it does not introduce any parameters to be learned.

2.1 Combining Area Features

Alternatively, we can derive a richer representation of each area by using features other than the mean of the key vectors of the area. For example, we can consider the standard deviation of the key vectors within each area.

$$\sigma_i = \sqrt{\frac{1}{|r_i|} \sum_{l=1}^{|r_i|} (k_{i,l} - \mu_i)^2} \tag{5}$$

We can also consider the height and width of each area, $h_i, 1 \leq h_i \leq H$ and $w_i, 1 \leq w_i \leq W$, as the features of the area. To combine these features, we use a multi-layer perceptron. To do so, we treat h_i and w_i as discrete values and project them onto a vector space using embedding (see Equation 6 and 7).

$$e_i^h = 1(h_i)E^h \tag{6}$$

$$e_i^w = 1(w_i)E^w \tag{7}$$

where $1(h_i)$ and $1(w_i)$ are the one-hot encoding of h_i and w_i, and $E^h \in R^{H \times S}$ and $E^w \in R^{W \times S}$ are the embedding matrices. S is the depth of the embedding. We concatenate them to form the representation of the shape of an area.

$$e_i = [e_i^h, e_i^w] \tag{8}$$

We then combine them using a single-layer perceptron followed by a linear transformation (see Equation 9).

$$k_i^r = \phi(\mu_i W_\mu + \sigma_i W_\sigma + e_i W_e) W_d \tag{9}$$

where ϕ is a nonlinear transformation such as ReLU, and $W_\mu \in \mathbb{R}^{D \times D}, W_\sigma \in \mathbb{R}^{D \times D}, W_e \in \mathbb{R}^{2S \times D}$ and $W_d \in \mathbb{R}^{D \times D}$. W_μ, W_σ, W_e and W_d are trainable parameters.

2.2 Fast Computation Using Summed Area Table

If we naively compute μ_i, σ_i and v_i^{Ti}, the time complexity for computing attention will be $O(|M|A^2)$ where $|M|$ is the size of the memory that is L for a 1-dimensional sequence or $L_v L_h$ for a 2-dimensional memory. A is the maximum size of an area, which is S in the one dimensional case and WH in the 2-dimensional case. This is computationally expensive in comparison to the attention computed on the original memory, which is $O(|M|)$. To address the issue, we use summed area table, an optimization technique that has been used in computer vision for computing features on image areas (Viola & Jones, 2001). It allows constant time to calculate a summation-based feature in each rectangular area, which allows us to bring down the time complexity to $O(|M|A)$.

Summed area table is based on a pre-computed integral image, I, which can be computed in a single pass of the memory (see Equation 10). Here let us focus on the area value calculation for a 2-dimensional memory because a 1-dimensional memory is just a special case with the height of the memory grid as 1.

$$I_{x,y} = v_{x,y} + I_{x,y-1} + I_{x-1,y} \tag{10}$$

Algorithm 1: Compute the vector sum and the size of each area, for all the qualified rectangular areas on a given grid.

Input: A tensor G in shape of $[H, W, D]$ that represents a grid with height H and width W where each item is a vector of depth D.

Output: Sum of vectors of each area, U, and height and width of each area, S_h and S_w.

Hyperparameter: maximum area width W_a and height H_a allowed.

1 Compute horizontal integral image I_h by cumulative sum along horizontal direction over G;
2 Compute integral image I_{hv} by cumulative sum along vertical directions over I_h;
3 Acquire I by padding all-zero vectors to the left and top of I_{hv};
4 **for** $h = 1, \cdots, H_a$ **do**
5   **for** $w = 1, \cdots, W_a$ **do**
6          $I_1 \leftarrow I[h + 1 :, w + 1 :, :]$;
7          $I_2 \leftarrow I[: -h - 1, : -w - 1, :]$;
8          $I_3 \leftarrow I[h + 1 :, : -w - 1, :]$;
9          $I_4 \leftarrow I[: -h - 1, w + 1 :, :]$;
10         $\bar{U} = I_1 + I_2 - I_3 - I_4$;
11         $\bar{S_h} \leftarrow [h]^{(H-h) \times (W-w)}$; Fill tensor with value h for the height of each area;
12         $\bar{S_w} \leftarrow [w]^{(H-h) \times (W-w)}$; Fill tensor with value w for the width of each area;
13         $S_h \leftarrow [S_h \ \bar{S_h}]$, reshape $\bar{S_h}$ to $[-1, 1]$ and concatenate on the first dimension;
14         $S_w \leftarrow [S_w \ \bar{S_w}]$, reshape $\bar{S_w}$ to $[-1, 1]$ and concatenate on the first dimension;
15         $U \leftarrow [U \ \bar{U}]$, reshape $\bar{U}$ to $[-1, D]$ and concatenate on the first dimension;
16 **return** U, S_h and S_w.

---

where x and y are the coordinates of the item in the memory. With the integral image, we can calculate the key and value of each area in constant time. The sum of all the vectors in a rectangular area can be easily computed as the following (Equation 11).

$$v_{x1,y1,x2,y2} = I_{x2,y2} + I_{x1,y1} - I_{x2,y1} - I_{x1,y2} \tag{11}$$

where $v_{x1,y1,x2,y2}$ is the value for the area located with the top-left corner at (x_1, y_1) and the bottom-right corner at (x_2, y_2). By dividing $v_{x1,y1,x2,y2}$ with the size of the area, we can easily compute $\mu_{x1,y1,x2,y2}$. Based on the summed area table, $\sigma^2_{x1,y1,x2,y2}$ (thus $\sigma_{x1,y1,x2,y2}$) can also be computed at constant time for each area (see Equation 12), where $I^2_{x,y} = v^2_{x,y} + I^2_{x,y-1} + I^2_{x-1,y}$, which is the integral image of the element-wise squared memory.

$$\sigma^2_{x1,y1,x2,y2} = \frac{I^2_{x2,y2} + I^2_{x1,y1} - I^2_{x2,y1} - I^2_{x1,y2}}{(x2 - x1) \times (y2 - y1)} - \mu^2_{x1,y1,x2,y2} \tag{12}$$

The core component for computing these quantities is to be able to quickly compute the sum of vectors in each area after we obtain the integral image table I for each coordinate $[x, y]$, as shown in Equation 10 and 11. We present the Pseudo code for performing Equation 10 and Equation 11 as well as the shape size of each area in Algorithm (1) and the code for computing the mean, sum and standard deviation (Equation 12) in Algorithm (2). These Pseudo code are designed based on Tensor operations, which can be implemented efficiently using libraries such as TensorFlow [1] and PyTorch [2].

3   EXPERIMENTS

We experimented with area attention on two important tasks: neural machine translation and image captioning, where attention has been an important component in these tasks. The architectures involves several popular encoder and decoder choices, such as LSTM (Hochreiter & Schmidhuber,

---

[1]https://github.com/tensorflow/tensorflow

[2]https://github.com/pytorch/pytorch

Algorithm 2: Compute the vector mean, standard deviation, and sum as well as the size of each area, for all the qualified rectangular areas on a grid.

Input: A tensor G in shape of $[H, W, D]$ that represents a grid with height H and width W where each item is a vector of depth D.

Output: Vector mean μ, standard deviation σ and sum U as well as height S_h and width S_w of each area.

1 Acquire U, S_h and S_w using Algorithm 1 with input G;
2 Acquire $U^{'}$ using Algorithm 1 with input $G \odot G$ where $\odot$ is for element-wise multiplication;
3 $\mu \leftarrow U \oslash S$ where $\oslash$ is for element-wise division;
4 $\mu^{'} \leftarrow U^{'} \oslash S$;
5 $\sigma \leftarrow \sqrt{\mu^{'} - \mu \odot \mu}$;
6 **return** μ, σ, U, as well as S_h and S_w.

1997) and Transformer (Vaswani et al., 2017). The attention mechansims in these tasks include both self attention and encoder-decoder attention.

3.1 Neural Machine Translation

We experimented with area attention on two model architectures. One is Transformer, a recent architecture (Vaswani et al., 2017) that has established the state of art performance on WMT 2014 English-to-German and English-to-French tasks. The model has not been used for character-level translation tasks that deals with much longer sequences. The other architecture is LSTM with encoder-decoder attention, which has been a popular choice for neural machine translation tasks. We experimented with the same datasets as the ones used in (Vaswani et al., 2017). In the WMT 2014 English-German dataset, there are about 4.5 million English-German sentence pairs, and in the English-French dataset, there are about 36 million English-French sentence pairs (Wu et al., 2016).

3.1.1 Transformer Experiments

Transformer heavily uses attentional mechanisms, including both self-attention in the encoder and the decoder, and attention from the decoder to the encoder. We vary the configuration of Transformer to investigate how area attention impacts the model. In particular, we experimented the following variations of Transformer: *Tiny* (#hidden layers=2, hidden size=128, filter size=512, #attention heads=4), *Small* (#hidden layers=2, hidden size=256, filter size=1024, #attention heads=4), and *Base* (#hidden layers=6, hidden size=512, filter size=2048, #attention heads=8). When using area attention, we applied area attention with the maximum area size of 5 to both encoder and decoder self-attention, and the encoder-decoder attention in the first two layers of Transformer.

During training, sentence pairs were batched together based on their approximate sequence lengths. Each training batch contained a set of sentence pairs that amount to approximately 32000 source and target tokens. A token can be a character for character-level translation, or a byte pair (Britz et al., 2017) or a word piece (Wu et al., 2016) that were used in the original Transformer experiments. We trained each of these models on one machine with 8 NVIDIA P100 GPUs for a total of 250,000 steps. All the training took less than 2 days to finish. Similar to previous work, we used the Adam optimizer with a varying learning rate over the course of training, as in (Vaswani et al., 2017) (see there for details).

We first examined the character-level English-to-German translation, because we speculate that area attention can help substantially due to the large number of items to be considered for attention. We found area attention consistently improved Transformer across all the model configurations. The best result we found in the literature is $BLEU = 22.62$ reported by (Wu et al., 2016). We achieved $BLEU = 25.03$ for the English-to-German character-level translation task and $BLEU = 33.69$ on the English-to-French character-level translation task. Note that these accuracy gains are based on the basic form of area attention (see Equation 3 and 4), which does not add any additional trainable parameters to the model.

Table 1: The BLEU scores on character-level translation tasks for the Transformer-based architecture with varying model capacities.

Model Configuration	Regular Attention		Area Attention (Eq.3 and 4)	
	EN-DE	EN-FR	EN-DE	EN-FR
Tiny	6.97	9.47	**7.39**	**11.79**
Small	12.18	18.75	**13.44**	**21.24**
Base	24.65	32.80	**25.03**	**33.69**

We then tested area attention on the token-level translation tasks. Area attention also improved Transformer on most model variations (see Table 2), although the gain is not as substantial as the one on the character-level translation tasks. Particularly, area attention achieved the BLEU scores of 28.17 (EN-DE) and 39.22 (EN-FR)—both improved upon the state-of-art results reported in (Vaswani et al., 2017): 27.3 (EN-DE) and 38.1 (EN-FR), for the Transformer base model.

Table 2: The BLEU scores on token-level translation tasks for the variations of the Transformer-based architecture.

Model Configuration	Regular Attention		Area Attention (Eq.3 and 4)	
	EN-DE	EN-FR	EN-DE	EN-FR
Tiny	18.60	27.07	**18.80**	**27.29**
Small	**22.80**	31.91	**22.80**	**32.28**
Base	27.96	39.10	**28.17**	**39.22**

3.1.2 LSTM EXPERIMENTS

For LSTM, we used a 2-layer LSTM for both its encoder and decoder. The encoder-decoder attention is based on multiplicative attention where the alignment of a query and a memory key is computed as their dot product (Luong et al., 2015). We vary the size of LSTM to investigate how area attention can improve LSTM on the character-level translation tasks. Compared to Transformer, LSTM trains quite slow. We trained each of these models on one machine with 8 NVIDIA P100 GPUs over three days. For the purpose of observing the impact of area attention on each LSTM configuration, rather than for competing with Transformer, we trained LSTM for 80000 iterations.

LSTM enhanced with area attention outperformed the baseline in most conditions (see Table 3) on both the English-to-German and English-to-French character-level translation tasks. The accuracy gain on the English-to-French task seems more pronounced.

Table 3: The Negative Log perplexity on predicting each character in a target sentence on validation data for the LSTM-based architecture with a varying number of LSTM cells. The larger the number is the better.

#LSTM Cells	Regular Attention		Area Attention (Eq.3 and 4)	
	EN-DE	EN-FR	EN-DE	EN-FR
256	-0.7984	-0.7770	**-0.7981**	**-0.7655**
512	-0.6506	-0.6343	**-0.6504**	**-0.6318**
1024	**-0.5585**	-0.5527	-0.5603	**-0.5521**

3.2 IMAGE CAPTIONING

Image captioning is the task to generate natural language description of an image that reflects the visual content of an image. This task has been addressed previously using a deep architecture that

features an image encoder and a language decoder (Xu et al., 2015; Sharma et al., 2018). The image encoder typically employs a convolutional net such as ResNet (He et al., 2015) to embed the images and then uses a recurrent net such as LSTM or Transformer (Sharma et al., 2018) to encode the image based on these embeddings. For the decoder, either LSTM (Xu et al., 2015) or Transformer (Sharma et al., 2018) has been used for generating natural language descriptions. In many of these designs, attention mechanisms have been an important component that allows the decoder to selectively focus on a specific part of the image at each step of decoding, which often leads to better captioning quality.

In this experiment, we follow a champion condition in the experimental setup of (Sharma et al., 2018) that achieved state-of-the-art results. It uses a pre-trained Inception-ResNet to generate 8×8 image embeddings, a 6-layer Transformer for image encoding and a 6-layer Transformer for decoding. The dimension of Transformer is 512 and the number of heads is 8. We intend to investigate how area attention improves the captioning accuracy, particularly regarding self-attention and encoder-decoder attention computed off the image, which resembles a 2-dimensional case for using area attention. We also vary the maximum area size allowed to examine the impact.

Similar to (Sharma et al., 2018), we trained each model based on the training & development sets provided by the COCO dataset (Lin et al., 2014), which as 82K images for training and 40K for validation. Each of these images have at least 5 groudtruth captions. The training was conducted on a distributed learning infrastructure (Dean et al., 2012) with 10 GPU cores where updates are applied asynchronously across multiple replicas. We then tested each model on the Flickr 1K (Young et al., 2014) test set, which is out-of-domain for the trained model. For each experiment, we report CIDEr (Vedantam et al., 2014) and ROUGE-L (Lin & Och, 2004) metrics. For both metrics, higher number means better captioning accuracy—the closer distances between the predicted and the groundtruth captions.

In the benchmark model, a regular multi-head attention is used (see the first row in Table 4). We then experimented with several variations by adding area attention with different maximum area sizes to the first 2 layers of the image encoder and the first 2 layers of the caption decoder. 2×2 stands for the maximum area size for the first two layers in the image encoder (a 2-dimensional case). $3 \times 3^*$ denotes the maximum area size and $*$ means the combined area features are used for the key (Equation 9). 2^* stands for 1 dimensional area attention for the caption decoder.

Table 4: Test accuracy of image captioning models that are trained on COCO and tested on Flickr. See the previous results of the benchmark model at the row "T2T8x8 COCO" in Table 7 of (Sharma et al., 2018).

Self & Enc-Dec Attention on Image	Self-Attention on Caption	ROUGE-L	CIDEr
Regular	Regular	0.409	0.355
2×2 Eq. 3	Regular	0.410	0.359
$3 \times 3^*$ Eq. 9	Regular	0.419	**0.367**
$3 \times 3^*$ Eq. 9	2^* Eq. 9	**0.421**	0.365

We found models with area attention outperformed the benchmark on both ROUGE-L and CIDEr metrics. The model with 2×2 does not use any additional parameters–the same number of parameters as the benchmark. The model with $3 \times 3^*$ and 2^* achieved the best results overall, which only added a small fraction of the number of parameters to the benchmark model. When comparing with the results reported in (Sharma et al., 2018) (Row "T2T8x8 COCO" in Table 7), our model still produced better accuracy.

4 CONCLUSIONS

In this paper, we present a novel attentional mechanism by allowing the model to attend to areas as a whole. An area contains one or a group of items in the memory to be attended. The items in the area are either spatially adjacent when the memory has 2-dimensional structure, such as images, or temporally adjacent for 1-dimensional memory, such as natural language sentences. Importantly, the size of an area, i.e., the number of items in an area, can vary depending on the learned coherence of the adjacent items, which gives the model the ability to attend to information at varying granularity. Area

attention contrasts with the existing attentional mechanisms that are item-based. We evaluated area attention on two tasks: neural machine translation and image captioning, based on model architectures such as Transformer and LSTM. On both tasks, we obtained new state-of-the-art results using area attention.

REFERENCES

Dzmitry Bahdanau, Kyunghyun Cho, and Yoshua Bengio. Neural machine translation by jointly learning to align and translate. *CoRR*, abs/1409.0473, 2014. URL http://arxiv.org/abs/1409.0473.

Denny Britz, Anna Goldie, Minh-Thang Luong, and Quoc V. Le. Massive exploration of neural machine translation architectures. *CoRR*, abs/1703.03906, 2017. URL http://arxiv.org/abs/1703.03906.

Jeffrey Dean, Greg S. Corrado, Rajat Monga, Kai Chen, Matthieu Devin, Quoc V. Le, Mark Z. Mao, Marc'Aurelio Ranzato, Andrew Senior, Paul Tucker, Ke Yang, and Andrew Y. Ng. Large scale distributed deep networks. In *Proceedings of the 25th International Conference on Neural Information Processing Systems*, NIPS'12, pp. 1223–1231, USA, 2012. Curran Associates Inc. URL http://dl.acm.org/citation.cfm?id=2999134.2999271.

Kaiming He, Xiangyu Zhang, Shaoqing Ren, and Jian Sun. Deep residual learning for image recognition. *CoRR*, abs/1512.03385, 2015. URL http://arxiv.org/abs/1512.03385.

Sepp Hochreiter and Jürgen Schmidhuber. Long short-term memory. *Neural Comput.*, 9(8):1735–1780, November 1997. ISSN 0899-7667. doi: 10.1162/neco.1997.9.8.1735. URL http://dx.doi.org/10.1162/neco.1997.9.8.1735.

Jason Lee, Kyunghyun Cho, and Thomas Hofmann. Fully character-level neural machine translation without explicit segmentation. *CoRR*, abs/1610.03017, 2016. URL http://arxiv.org/abs/1610.03017.

Chin-Yew Lin and Franz Josef Och. Orange: A method for evaluating automatic evaluation metrics for machine translation. In *Proceedings of the 20th International Conference on Computational Linguistics*, COLING '04, Stroudsburg, PA, USA, 2004. Association for Computational Linguistics. doi: 10.3115/1220355.1220427. URL https://doi.org/10.3115/1220355.1220427.

Tsung-Yi Lin, Michael Maire, Serge J. Belongie, Lubomir D. Bourdev, Ross B. Girshick, James Hays, Pietro Perona, Deva Ramanan, Piotr Dollár, and C. Lawrence Zitnick. Microsoft COCO: common objects in context. *CoRR*, abs/1405.0312, 2014. URL http://arxiv.org/abs/1405.0312.

Minh-Thang Luong, Hieu Pham, and Christopher D. Manning. Effective approaches to attention-based neural machine translation. *CoRR*, abs/1508.04025, 2015. URL http://arxiv.org/abs/1508.04025.

Marco Pedersoli, Thomas Lucas, Cordelia Schmid, and Jakob Verbeek. Areas of attention for image captioning. *CoRR*, abs/1612.01033, 2016. URL http://arxiv.org/abs/1612.01033.

Piyush Sharma, Nan Ding, Sebastian Goodman, and Radu Soricut. Conceptual captions: A cleaned, hypernymed, image alt-text dataset for automatic image captioning. In *Proceedings of the 56th Annual Meeting of the Association for Computational Linguistics, ACL 2018, Melbourne, Australia, July 15-20, 2018, Volume 1: Long Papers*, pp. 2556–2565, 2018. URL https://aclanthology.info/papers/P18-1238/p18-1238.

Ashish Vaswani, Noam Shazeer, Niki Parmar, Jakob Uszkoreit, Llion Jones, Aidan N. Gomez, Lukasz Kaiser, and Illia Polosukhin. Attention is all you need. *CoRR*, abs/1706.03762, 2017. URL http://arxiv.org/abs/1706.03762.

Ramakrishna Vedantam, C. Lawrence Zitnick, and Devi Parikh. Cider: Consensus-based image description evaluation. *CoRR*, abs/1411.5726, 2014. URL http://arxiv.org/abs/1411.5726.

Paul Viola and Michael Jones. Rapid object detection using a boosted cascade of simple features. pp. 511–518, 2001.

Yonghui Wu, Mike Schuster, Zhifeng Chen, Quoc V. Le, Mohammad Norouzi, Wolfgang Macherey, Maxim Krikun, Yuan Cao, Qin Gao, Klaus Macherey, Jeff Klingner, Apurva Shah, Melvin Johnson, Xiaobing Liu, Lukasz Kaiser, Stephan Gouws, Yoshikiyo Kato, Taku Kudo, Hideto Kazawa, Keith Stevens, George Kurian, Nishant Patil, Wei Wang, Cliff Young, Jason Smith, Jason Riesa, Alex Rudnick, Oriol Vinyals, Greg Corrado, Macduff Hughes, and Jeffrey Dean. Google's neural machine translation system: Bridging the gap between human and machine translation. *CoRR*, abs/1609.08144, 2016. URL `http://arxiv.org/abs/1609.08144`.

Kelvin Xu, Jimmy Ba, Ryan Kiros, Kyunghyun Cho, Aaron C. Courville, Ruslan Salakhutdinov, Richard S. Zemel, and Yoshua Bengio. Show, attend and tell: Neural image caption generation with visual attention. *CoRR*, abs/1502.03044, 2015. URL `http://arxiv.org/abs/1502.03044`.

P Young, A Lai, M Hodosh, and Julia Hockenmaier. From image descriptions to visual denotations: New similarity metrics for semantic inference over event descriptions. 2:67–78, 01 2014.